This is a repository copy of *A micro-inertia gradient visco-elastic motivation for proportional damping*.

White Rose Research Online URL for this paper:
http://eprints.whiterose.ac.uk/85969/

Version: Accepted Version

Article:

A micro-inertia gradient visco-elastic motivation for proportional damping

C. Bagni[a,*], I. Gitman[b,*], H. Askes[a]

[a]*University of Sheffield, Department of Civil and Structural Engineering, Mappin Street, Sheffield S1 3JD, United Kingdom*
[b]*University of Sheffield, Department of Mechanical Engineering, Mappin Street, Sheffield S1 3JD, United Kingdom*

Abstract

In this paper, a micro-inertia gradient visco-elasticity theory is proposed and implemented for the description of wave dispersion in periodic visco-elastic composites characterised by (stiffness-)proportional damping. An expression for the internal length parameter has been derived in terms of geometry and material properties. The theory has been validated through a numerical simulation of wave propagation in a one-dimensional periodic composite bar for two different heterogeneity levels, where the proposed theory has shown good agreement with the solution obtained by explicitly modelling the material heterogeneity. The effects of both gradient enrichment and viscosity on wave propagation as well as their interaction have also been analysed.

Keywords: Gradient viscoelasticity, Generalised continuum, Internal length scale, Proportional damping

*Corresponding author. Tel.:+44(0)114 2227728; fax:+44(0)114 2227890
Email addresses: `c.bagni@sheffield.ac.uk` (C. Bagni),
`i.gitman@sheffield.ac.uk` (I. Gitman), `h.askes@sheffield.ac.uk` (H. Askes)

1. Introduction

Many gradient-enriched theories have been proposed in the past to overcome deficiencies of classical elasticity (see for instance [1–3]) and plasticity [4–7] theories in describing particular phenomena in both static and dynamics, such as size effects, strain and stress fields in the neighbourhood of crack tips and dislocation lines [2, 3, 8–12] and wave dispersion in dynamics [13–16].

The failure of classical theories in the description of the previously mentioned phenomena is due to the absence of internal length parameters, characteristic of the underlying microstructure. On the contrary, gradient-enriched theories are capable of considering the effects of microstructure on the macroscopic behaviour of a material by including high-order gradients, accompanied by internal length parameters, which are representative of the microstructure. Despite the significant number of gradient-enriched theories for elasticity and plasticity, gradient visco-elasticity theories have received less interest in the past. In particular, materials like synthetic polymers, biopolymers, wood, human tissues, bituminous materials and metals at high temperature show strong visco-elastic behaviours, thus it is of interest to develop a continuum theory that captures the micro-structural as well as the time-dependent phenomena.

An attempt to describe viscoelastic materials has been made by Gudmundson [17] in 2006, who proposed a strain gradient visco-elastic model to describe length scale effects in such materials. However, as the author points himself further in [17], the proposed method is lacking a link between the length scale and the material's microstructure.

2

In this paper a micro-inertia gradient visco-elasticity theory is proposed to study wave dispersion in periodic composites; allowing new insights about the effects of both gradient enrichment and viscosity on wave propagation as well as their interaction. The proposed theory is characterised by a direct link with the underlying microstructure as well as material properties. Moreover, an effective and straightforward finite element implementation of the presented theory is proposed. In Section 2, derivation of the continuum high-order model, characterised by an internal length parameter, is presented starting from a simple periodic discrete lattice model. In Section 3 the higher accuracy of the proposed methodology in capturing the dispersive behaviour of the discrete model is shown through a dispersion analysis. Thereafter, in Section 4 a brief description of the finite element implementation of the proposed theory is provided, along with some details about the adopted time integration algorithm. In Section 5 a homogenisation approach for periodic composites is proposed, along with a relation for the internal length scale, linking geometry and material properties. In Section 6 an application of the new methodology is presented, in order to show the interaction between viscosity and inertia gradients, as well as the different effects they have on wave propagation and dispersion. Finally, some final considerations about the gradient visco-elastic theory are given in Section 7, followed by a discussion of future research directions.

2. Model derivation

Gradient visco-elasticity theory can be obtained through the continualisation of a discrete lattice (Fig. 1) as explained in [18], taking into account

that now the particles of mass m are in series with Kelvin-Voigt models characterised by spring stiffness s and viscosity η; the distance between two consecutive particles is denoted d. The equation of the motion of the nth particle can be written as:

$$m\ddot{u}_n = s\left(u_{n+1} - 2u_n + u_{n-1}\right) + \eta\left(\dot{u}_{n+1} - 2\dot{u}_n + \dot{u}_{n-1}\right) \tag{1}$$

Passing now from the discrete to the continuum model, the displacements can be rewritten with the following expressions:

$$u(x,t) = u_n(t) \qquad \text{and} \qquad u(x \pm d, t) = u_{n\pm 1}(t) \tag{2}$$

Then, by using the Taylor series the generic displacement can be written as

$$u(x \pm d, t) \approx u(x,t) \pm du'(x,t) + \frac{1}{2}d^2 u''(x,t) \pm \frac{1}{6}d^3 u'''(x,t) +$$
$$+ \frac{1}{24}d^4 u''''(x,t) \pm \cdots \tag{3}$$

and substituting Eq. (3) into Eq. (1), a new equation of the motion is obtained, in which an higher order term appears for both displacements and velocities:

$$m\ddot{u}(x,t) = sd^2\left[u''(x,t) + \frac{1}{12}d^2 u''''(x,t)\right] +$$
$$+ \eta d^2\left[\dot{u}''(x,t) + \frac{1}{12}d^2 \dot{u}''''(x,t)\right] \tag{4}$$

or similarly, replacing the mass, the spring stiffness and the (stiffness-) proportional damping, respectively, with the following relations $m = \rho A d$, $s = EA/d$ and $\eta = \tau EA/d$

4

$$\rho \ddot{u}(x,t) = E\left[u''(x,t) + \frac{1}{12}d^2 u''''(x,t) + \tau\left(\dot{u}''(x,t) + \frac{1}{12}d^2 \dot{u}''''(x,t)\right)\right] \quad (5)$$

where ρ is the mass density, E is the Young's modulus and τ is the (stiffness-) proportional damping coefficient. In Eqs. (4) and (5), truncation of the Taylor series has been applied such that only the next-highest order terms are maintained.
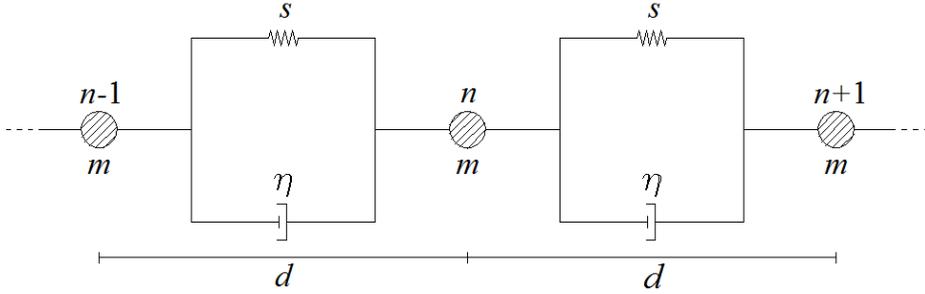

Figure 1. Mono-dimensional discrete model consisting in particles and Kelvin-Voigt models.

In this way an enriched-gradient model with positive sign has been obtained, which unfortunately has been proved to produce unstable results [19]. On the other hand, as shown in [19] the same model but with negative sign leads to stable results. This can be obtained trough a simple mathematical manipulation that consists in taking the Laplacian of the original equation of the motion (5), that is (ignoring the spatial and temporal dependence for notational simplicity)

$$\rho \ddot{u}'' = E\left[u'''' + \frac{1}{12}d^2 u'''''' + \tau\left(\dot{u}'''' + \frac{1}{12}d^2 \dot{u}''''''\right)\right] \quad (6)$$

multiplying Eq. (6) by $\frac{1}{12}d^2$, which leads to (neglecting higher-order terms)

$$\frac{1}{12}d^2\rho\ddot{u}'' = \frac{1}{12}d^2E\left(u'''' + \tau\dot{u}''''\right) \tag{7}$$

and finally subtracting Eq. (7) from Eq. (5), which leads to:

$$\rho\left(\ddot{u} - \frac{1}{12}d^2\ddot{u}''\right) = E\left(u'' + \tau\dot{u}''\right) \tag{8}$$

or alternatively

$$\rho\left(\ddot{u} - \ell^2\ddot{u}''\right) = E\left(u'' + \tau\dot{u}''\right) \tag{9}$$

where the length scale ℓ is linked to the inter-particle distance d by the expression $\ell = \frac{1}{\sqrt{12}}d$.

This technique can also be applied in multi-dimensions, which in the isotropic case leads to the following equation of the motion:

$$\rho\left(\ddot{\mathbf{u}} - \ell^2\nabla^2\ddot{\mathbf{u}}\right) = \mathbf{L}^T\mathbf{D}\mathbf{L}\left(\mathbf{u} + \tau\dot{\mathbf{u}}\right) \tag{10}$$

where $\mathbf{D}$ is the constitutive matrix and the derivative operators $\mathbf{L}$ and ∇, in the most general case, take the form

$$\mathbf{L} = \begin{bmatrix} \frac{\partial}{\partial x} & 0 & 0 \\ 0 & \frac{\partial}{\partial y} & 0 \\ 0 & 0 & \frac{\partial}{\partial z} \\ \frac{\partial}{\partial y} & \frac{\partial}{\partial x} & 0 \\ \frac{\partial}{\partial z} & 0 & \frac{\partial}{\partial x} \\ 0 & \frac{\partial}{\partial z} & \frac{\partial}{\partial y} \end{bmatrix} \quad \text{and} \quad \nabla = \begin{bmatrix} \frac{\partial}{\partial x} \\ \frac{\partial}{\partial y} \\ \frac{\partial}{\partial z} \end{bmatrix} \quad \text{with} \quad \nabla^2 \equiv \nabla^T\nabla \tag{11}$$

6

Note 1. For non-isotropic materials the length scale ℓ is not a scalar anymore, but the length scale effects in each direction of anisotropy are collected in a tensor $\mathbf{L_s}$ (see for example [20]).

3. Dispersion analysis

3.1. Discrete model

To study the dispersive behaviour of the discrete model of Eq. (1), the general harmonic solution

$$u_n = U \exp(\mathrm{i}(\omega t - kx_n)) \tag{12}$$

is considered, where U is the amplitude, k is the wave number, t is the time, x_n the coordinate of the nth particle and ω is the angular frequency defined as a complex number as

$$\omega = \omega_h + \mathrm{i}\omega_d \tag{13}$$

with ω_h and ω_d the harmonic and damping component of ω, respectively.

Substituting Eqs. (12) and (13) into Eq. (1) and considering that $x_{n\pm1} = x_n \pm d$, the following expression for ω_d and ω_h are obtained

$$\omega_d = 2\frac{c_e^2}{d^2}\tau \sin^2\left(\frac{kd}{2}\right) \tag{14}$$

$$\omega_h = 2\frac{c_e}{d}\left|\sin\left(\frac{kd}{2}\right)\right|\sqrt{1 - \frac{c_e^2}{d^2}\tau^2 \sin^2\left(\frac{kd}{2}\right)} \tag{15}$$

where $c_e = \sqrt{E/\rho}$ is the elastic bar velocity. Sub-critical damping is identified via non-imaginary values of ω_h, which leads to the following condition:

7

$$1 - \frac{c_e^2}{d^2}\tau^2 \sin^2\left(\frac{kd}{2}\right) \geq 0 \tag{16}$$

or in terms of τ:

$$\tau \leq \frac{1}{\left|\sin\left(\frac{kd}{2}\right)\right|}\frac{d}{c_e} \tag{17}$$

Since $0 \leq \left|\sin\left(\frac{kd}{2}\right)\right| \leq 1$, Eq. (17) can be simplified as

$$\tau \leq \frac{d}{c_e} \tag{18}$$

which sets the threshold value of τ that separates sub-critical and super-critical damping.

3.2. Continuum model

For what concerns the continuum model, the following harmonic solution

$$u(x,t) = U\exp(\mathrm{i}(\omega t - kx)) \tag{19}$$

is substituted into the one-dimensional continuum equation of the motion (8), leading to the following equation

$$\rho\omega^2\left(1 + \frac{1}{12}d^2k^2\right) = Ek^2\left(1 + \mathrm{i}\omega\tau\right) \tag{20}$$

Introducing Eq. (13) in Eq. (20) the following expressions for ω_d and ω_h are obtained:

$$\omega_d = \frac{c_e^2 k^2 \tau}{2\left(1 + \frac{1}{12}d^2k^2\right)} \tag{21}$$

$$\omega_h = \frac{c_e k}{\sqrt{1 + \frac{1}{12}d^2k^2}}\sqrt{1 - \frac{c_e^2 k^2 \tau^2}{4\left(1 + \frac{1}{12}d^2k^2\right)}} \tag{22}$$

8

Taking $d = 0$ m the continuum model for classical visco-elasticity is retrieved, obtaining the following expression for the harmonic component of the angular frequency

$$\omega_h = c_e k \sqrt{1 - \frac{c_e^2 k^2 \tau^2}{4}} \tag{23}$$

Thus,

$$\tau = 2 \frac{1}{c_e k_c} \tag{24}$$

is the condition for critical damping, from which can be easily determined the cut-off value k_c (i.e. the wave number associated with $\omega_h = 0$).
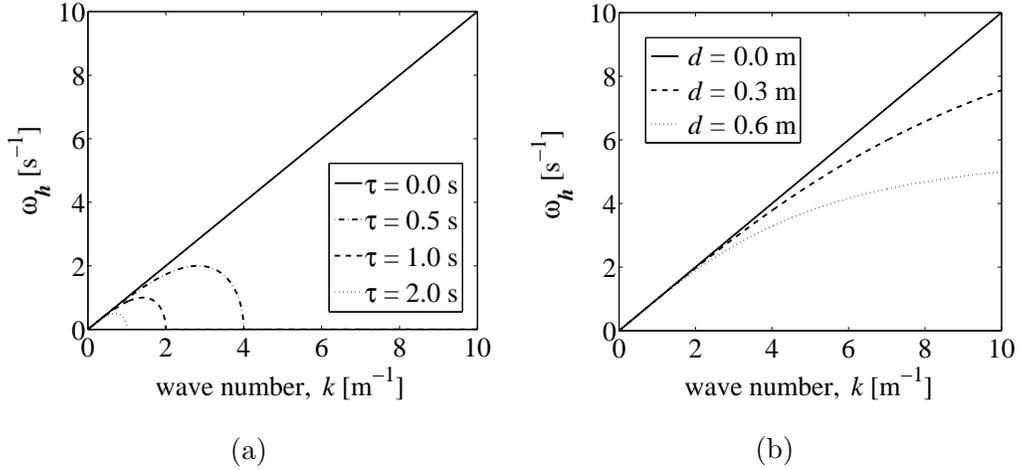

Figure 2. Harmonic component of the angular frequency versus wave number when classical visco-elasticity theory is applied (a) and for the non-viscous micro-inertia theory (b).

Similarly, the micro-inertia gradient elasticity model is found by setting

9

the condition $\tau = 0$ s which yields

$$\omega_h = \frac{c_e k}{\sqrt{1 + \frac{1}{12} d^2 k^2}} \qquad (25)$$

In Fig. 2a the harmonic component of the angular frequency ω_h is plotted against the wave number k, in the case the classical visco-elasticity theory is applied, for different values of τ, while in Fig. 2b the same graph is plotted for the non-viscous micro-inertia theory ($\tau = 0$ s), for different values of d.

Returning to Eq. (22), it can be observed that positive values of the argument of the second square root lead to real values of ω_h, while if the considered argument is negative, ω_h becomes imaginary. Considering Eq. (19) together with Eq. (13) it can be easily found that real values of ω_h lead to the case of sub-critical damping, while imaginary values make the system super-critically damped (see AppendixA for a more detailed discussion about the stability of this solution). Hence, summarising it can be stated that the condition

$$\tau_c = \frac{1}{\sqrt{3}} \frac{d}{c_e} \qquad (26)$$

which makes the argument of the square root null for $k \to \infty$, represents the condition of critical damping and consequently if $\tau < \tau_c$ the system is under-damped, while for $\tau > \tau_c$ a range of higher wave numbers will be over-damped.

Thus, an important feature of the proposed theory can be found in the fact that varying τ (which depends on material properties) it is possible to have control on which wave numbers are over-damped. In particular, the lower bound of the over-damped wave numbers can be defined as the cut-off

value k_c obtained by imposing

$$1 - \frac{c_e^2 k^2 \tau^2}{4 \left(1 + \frac{1}{12} d^2 k^2\right)} = 0 \qquad (27)$$

which leads to

$$k_c = \frac{2}{\sqrt{c_e^2 \tau^2 - \frac{1}{3} d^2}} \qquad (28)$$

that represents the wave number in correspondence of which ω_h is zero and beyond which imaginary frequencies ω_h are obtained.

In Fig. 3 the harmonic component of the angular frequency ω_h, obtained by applying the different models, is plotted versus the wave number k, for different values of the dimensionless parameter ξ, writing τ as

$$\tau = \xi \frac{d}{c_e} \qquad (29)$$

It is worth clarifying that the results shown in Fig. 3 are physically of interest only for $0 \leq k \leq \pi$ (i.e. first Brillouin zone). However, for reasons of completeness and to allow further mathematical considerations, expressed later in this Section, a wider range of wave numbers has been considered.

From Fig. 3, considering wave numbers up to π, it is evident that the micro-inertia gradient visco-elastic model is able to describe with higher accuracy the dispersive behaviour of the discrete model, compared to the classical visco-elastic model, even if it must be observed that the improvement introduced by the gradient enrichment becomes weaker for high value of τ.

It can also be noticed that, in the case of critical damping (Fig. 3b), the $\omega_h - k$ curve, resulting from the micro-inertia gradient model, can be split
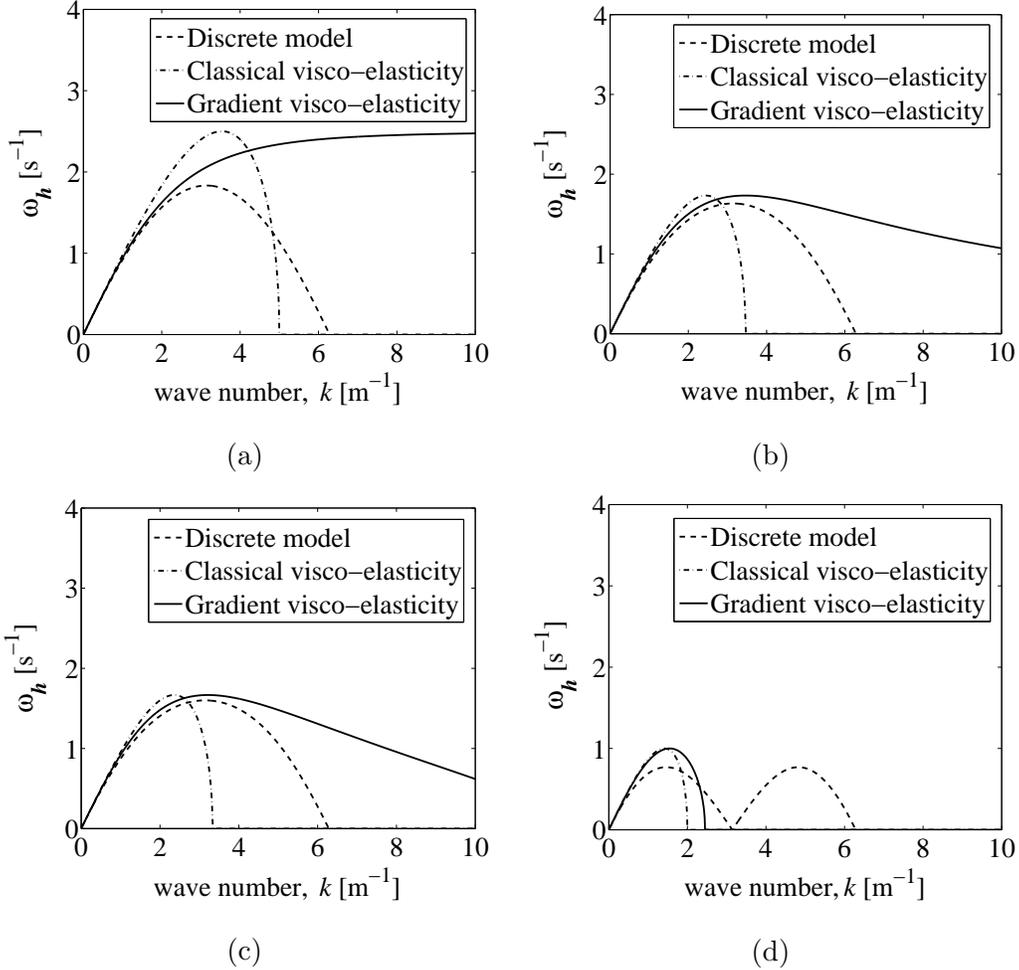
11

Figure 3. Harmonic component of the angular frequency versus wave number for the discrete model (dashed line), classical visco-elastic model (dash-dotted line) and micro-inertia gradient visco-elastic model (solid line), for different values of ξ: $\xi = 0.4$ (a), $\xi = 1/\sqrt{3}$ (b), $\xi = 0.6$ (c), $\xi = 1.0$ (d).

into two parts: a first part characterised by a negative second derivative (concave) and a second one convex. Through a more accurate study of the second derivative it has been found that for $\xi > 1/\sqrt{6}$ the curve shows an

inflexion point.

Thus, we can summarise the results of the proposed micro-inertia gradient model as follows

- $0 \leq \xi \leq 1/\sqrt{6}$: the $\omega_h - k$ curve is always concave and it tends to the horizontal asymptote

$$\omega_h = 6\frac{Ce}{d}\sqrt{\frac{1}{3} - \xi^2} \tag{30}$$

- $1/\sqrt{6} < \xi \leq 1/\sqrt{3}$: the curve is characterised by a first concave part followed by a second convex one, but ω_h is real for every wave number;

- $\xi > 1/\sqrt{3}$: ω_h assumes imaginary values for some wave numbers.

Finally, comparing Fig. 3 with Fig. 2 it can be easily seen that both classical visco-elasticity and gradient elasticity models alone are not able to accurately describe the dispersive behaviour of the discrete model, but introducing a micro-inertia gradient enrichment into the classical visco-elasticity theory a significant improvement of the results is obtained for $0 \leq k \leq \pi$.

4. Discretisation

Starting from Eq. (10) the finite element equations for the bi-dimensional case will be defined, while the equations for the three-dimensional case can be easily obtained, following a similar procedure. Some information about the time integration algorithm adopted in the proposed methodology to solve the equations of the motion will be also provided.

4.1. Finite element equations

The continuum displacements field is discretised by means of shape functions which, as usual, are collected in the matrix $\mathbf{N_u}$

$$\mathbf{N_u} = \begin{bmatrix} N_1 & 0 & N_2 & 0 & \cdots \\ 0 & N_1 & 0 & N_2 & \cdots \end{bmatrix} \tag{31}$$

which allow us to express the continuum displacements $\mathbf{u} = [u_x, u_y]^T$ in terms of the nodal displacements $\mathbf{d} = [d_{1x}, d_{1y}, d_{2x}, d_{2y}, \dots]^T$ through the relation $\mathbf{u} = \mathbf{N_u d}$.

Taking the weak form of the equation of the motion (10), considering now also the body forces $\mathbf{b}$, with domain Ω and boundary Γ, followed by integration by parts, and considering the discretisation of the displacements described above, we obtain the following equation:

$$\int_\Omega \rho \left[\mathbf{N_u}^T \mathbf{N_u} + \ell^2 \left(\frac{\partial \mathbf{N_u}^T}{\partial x} \frac{\partial \mathbf{N_u}}{\partial x} + \frac{\partial \mathbf{N_u}^T}{\partial y} \frac{\partial \mathbf{N_u}}{\partial y} \right) \right] \mathrm{d}\Omega \ \ddot{\mathbf{d}} +$$
$$+ \int_\Omega \mathbf{B_u}^T \mathbf{D} \mathbf{B_u} \mathrm{d}\Omega \ \left(\mathbf{d} + \tau \dot{\mathbf{d}} \right) = \int_\Omega \mathbf{N_u}^T \mathbf{b} \mathrm{d}\Omega + \int_\Gamma \mathbf{N_u}^T \mathbf{t} \mathrm{d}\Gamma \tag{32}$$

where $\mathbf{t}$ is the vector of the prescribed traction on the Neumann part of the boundary and includes also the inertia effects, while $\mathbf{B_u} = \mathbf{L N_u}$ is the strain-displacement matrix.

Finally we obtain the discrete system of equation

$$[\mathbf{M} + \mathbf{H}] \ddot{\mathbf{d}} + \mathbf{K} \left(\mathbf{d} + \tau \dot{\mathbf{d}} \right) = \mathbf{f} \tag{33}$$

with

$$\mathbf{K} = \int_\Omega \mathbf{B_u}^T \mathbf{D} \mathbf{B_u} \mathrm{d}\Omega \tag{34}$$

14

the stiffness matrix,

$$\mathbf{M} = \int_{\boldsymbol{\Omega}} \rho \mathbf{N_u}^T \mathbf{N_u} d\Omega \tag{35}$$

the classic mass matrix,

$$\mathbf{H} = \int_{\boldsymbol{\Omega}} \rho \gamma \ell^2 \left(\frac{\partial \mathbf{N_u}^T}{\partial x} \frac{\partial \mathbf{N_u}}{\partial x} + \frac{\partial \mathbf{N_u}^T}{\partial y} \frac{\partial \mathbf{N_u}}{\partial y} \right) d\Omega \tag{36}$$

the gradient-enriched part of the mass matrix and

$$\mathbf{f} = \int_{\boldsymbol{\Omega}} \mathbf{N_u}^T \mathbf{b} d\Omega + \int_{\Gamma} \mathbf{N_u}^T \mathbf{t} d\Gamma \tag{37}$$

the force vector.

4.2. Time integration

In dynamics the equations of the motion of discrete systems are solved in the time domain by using direct integration algorithms.

Here, the Crank-Nicolson method [21] has been used, obtained from the Newmark method [22] by setting the two parameters $\beta^* = 1/4$ and $\gamma^* = 1/2$, which is unconditionally stable [23].

The fundamental relations of this method are:

$$\ddot{u}_{i+1} = \frac{4}{\Delta t^2} \left(u_{i+1} - u_i - \Delta t \ \dot{u}_i - \frac{1}{4} \Delta t^2 \ddot{u}_i \right) \tag{38}$$

$$\dot{u}_{i+1} = \dot{u}_i + \frac{1}{2} \Delta t \left(\ddot{u}_i + \ddot{u}_{i+1} \right) \tag{39}$$

where u_i, $\dot{u}_i$ and $\ddot{u}_i$ are, respectively, the displacement, velocity and acceleration at the ith time instant, while Δt is the chosen time step; that lead to the following time-discretisation of Eq. (33)

15

$$\left[\frac{4\left[\mathbf{M}+\mathbf{H}\right]}{\Delta t^2} + \left(\frac{2\tau}{\Delta t} + 1 \right) \mathbf{K} \right] \mathbf{u}_{i+1} =$$

$$= \left[\mathbf{M}+\mathbf{H}\right] \left(\frac{4\mathbf{u}_i}{\Delta t^2} + \frac{4\dot{\mathbf{u}}_i}{\Delta t} + \ddot{\mathbf{u}}_i \right) + \tau \mathbf{K} \left(\frac{2\mathbf{u}_i}{\Delta t} + \dot{\mathbf{u}}_i \right) + \mathbf{f} \qquad (40)$$

from which the nodal displacements at time i+1 can be determined, knowing the values of the nodal displacements, velocities and accelerations at the previous time step i.

5. Homogenisation approach and length scale identification for periodic composites

In the scope of this paper, the periodic elastic composite analysed by [14] will be considered. This periodic composite consists of two different materials (properties are denoted by the subscript 1 and 2 respectively), with volume fraction defined by the parameter α as shown in Fig. 4.
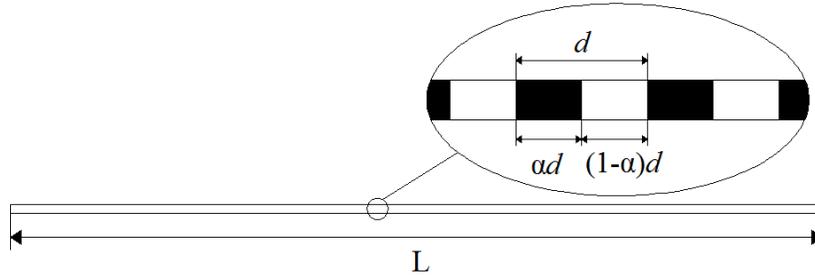

Figure 4. Mono-dimensional representation of a periodic bi-component material.

Now the constitutive relations can be presented as

$$\sigma = E \left(\varepsilon + \tau \dot{\varepsilon} \right) \qquad (41)$$

16

where τ is the damping proportional factor.

Considering the homogeneous continuum model proposed by [14], neglecting the multiple time scales and taking into account the constitutive relation (41), the leading order equation of the motion takes the following form:

$$\overline{\rho}\ddot{u} = \overline{E}\left(u'' + \tau\dot{u}''\right) \tag{42}$$

where

$$\overline{\rho} = \alpha\rho_1 + (1-\alpha)\rho_2 \tag{43}$$

$$\overline{E} = \frac{E_1 E_2}{(1-\alpha)E_1 + \alpha E_2} \tag{44}$$

are, respectively, the homogenised mass density and Young's modulus.

Including the next high-order term the equation of the motion reads:

$$\overline{\rho}\ddot{u} = \overline{E}\left(u'' + \tau\dot{u}''\right) + \gamma d^2 \overline{E}\left(u'''' + \tau\dot{u}''''\right) \tag{45}$$

where d is the size of the unit cell as shown in Fig. 4 and γ is expressed in the following way:

$$\gamma = \frac{1}{12}\left[\frac{\alpha(1-\alpha)(\rho_1 E_1 - \rho_2 E_2)}{(1-\alpha)\overline{\rho}E_1 + \alpha\overline{\rho}E_2}\right]^2 \tag{46}$$

Imposing the two conditions $0 < \alpha < 1$ and $\rho_1 E_1 \neq \rho_2 E_2$ we get $\gamma > 0$.

As it can be easily noticed, Eq. (45) represents an enriched-gradient equation of the motion in which the higher-gradient term is characterised by a positive sign, which, as previously mentioned, produces unstable results. However, with a mathematical procedure similar to the one previously explained, as also proposed by [14] for elastic materials, it is possible to replace the previous unstable model with a stable inertia-gradient model. This

17

mathematical manipulation consists in taking the second spatial derivative of Eq. (42), multiplying it by γd^2 and substituting the result into Eq. (45), which leads to the following stable inertia-gradient equation of the motion:

$$\overline{\rho}\left(\ddot{u} - \gamma d^2 \ddot{u}''\right) = \overline{E}\left(u'' + \tau \dot{u}''\right) \tag{47}$$

or equivalently

$$\overline{\rho}\left(\ddot{u} - \gamma d^2 \ddot{u}''\right) = \overline{E} u'' + \overline{C} \dot{u}'' \tag{48}$$

where $\overline{C} = \tau \overline{E}$.

Comparing now Eq. (9) with Eq. (48), the length scale ℓ can be written in terms of geometry and material parameters only:

$$\ell = d\sqrt{\gamma} \tag{49}$$

6. Numerical tests

The proposed theory has first been applied to the one-dimensional wave propagation problem consisting in a 100 m long periodic composite bar, similar to the one shown in Fig. 4, in which the first material is characterised by mass density ρ_1 and Young's modulus E_1, while for what concerns the second material, the properties are denoted as ρ_2 and E_2. Following Eqs. (43) and (44), the macroscopic effective material properties are $\overline{\rho} = 1$ kg m^{-3} and $\overline{E} = 1$ N m^{-2}. Both materials are characterised by the same damping proportional factor τ and the volume fraction is assumed to be $\alpha = 0.5$, while the unit cell size is taken $d = 1$ m.

The bar has a square cross section A $= 1$ m^2, it is fully restrained at its right hand end and subjected to a unit-pulse at its left hand end.
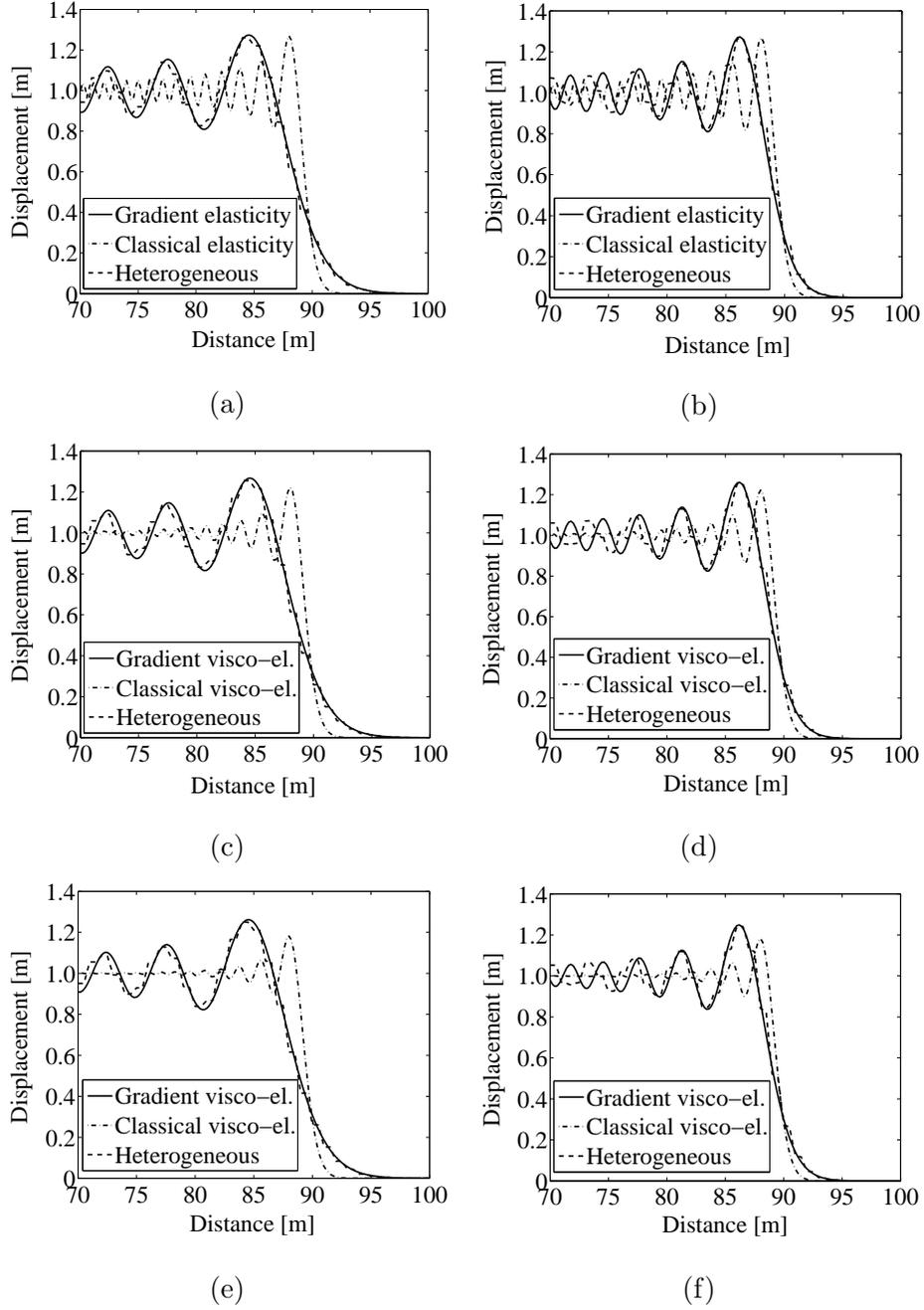
18

Figure 5. Dynamic response of the mono-dimensional periodic composite bar for Case a (a, c, e) and Case b (b, d, f) and for different value of the (stiffness-)proportional damping coefficient: $\tau = 0.000$ s (a, b), $\tau = 0.001$ s (c, d), $\tau = 0.002$ s (e, f), at $t = 90$ s.

19

The two problems presented in [24], denoted as Case a and Case b, are analysed for different values of τ ($\tau = 0.000$ s which corresponds to the case of rate independent elastic material discussed in [24], $\tau = 0.001$ s and $\tau = 0.002$ s). The length scales for the two problems are determined through Eqs. (46) and (49), which leads to $\ell = d\sqrt{\gamma} = 0.289$ m for Case a and $\ell = d\sqrt{\gamma} = 0.159$ m for Case b.

The problems have been modelled using linear elements, in particular the elastic/viscoelastic heterogeneous solution has been obtained by explicitly modelling the microstructural heterogeneity of the bar, through alternating groups of elements, characterised by the properties of material 1 and 2, so that the unit cell size $d = 1$ m. A time step of $\Delta t = 6.25 \cdot 10^{-2}$ s has been used for the heterogeneous solution, while for the classical and gradient simulations it has been assigned a value $\Delta t = 0.2$ s.

In Fig. 5 the wave front profile after 90 s is shown for both Case a and b and for different value of viscosity, where Figs. 5a and 5b are the same presented in [24]. Comparing the wave fronts produced by the gradient and the explicit heterogeneous models, it can be observed that the proposed theory provide a good approximation of the heterogeneous model. Furthermore, the comparison between the solution given by the gradient model with that resulting from classical elasticity (which, neglecting numerical dispersions, can be considered a Heaviside function) clearly shows the ability of the gradient enrichment to properly describe the dispersive behaviour of an heterogeneous material regardless the viscosity, in fact from Fig. 6 it can be noticed that viscosity does not produce any significant reduction in the speed propagation of the wave front, represented by the slope of the front itself. Fig. 5, finally,

20

shows that the dispersive character of a medium is led by the intensity of its heterogeneity, this means that the higher the ratios E_1/E_2 and ρ_1/ρ_2 (and consequently the value of the length scale ℓ) the stronger the dispersive effect of the medium.
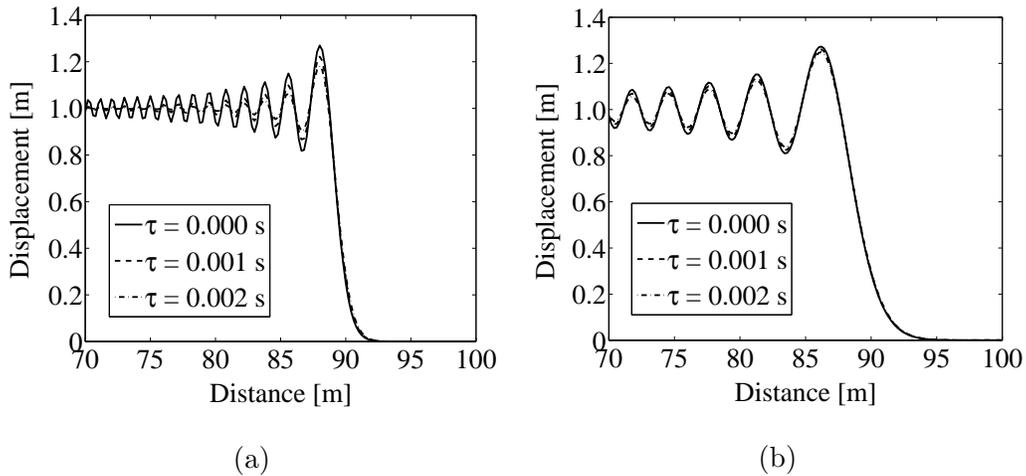

Figure 6. Effect of viscosity on the dynamic response of the bar: classical (a) and gradient (b) elastic/viscoelastic solutions for the Case b heterogeneous bar.

While Fig. 5 points out the effects and advantages of the gradient enrichment, from Fig. 6 it is possible to appreciate the effect of viscosity on the dynamic response of the bar, which mainly consists in a reduction of the amplitude of the high frequency components. This effect is particularly visible in the classical case, while introducing a certain heterogeneity of the material the effect becomes weaker and, as can be observed in Fig. 7, also this effect is led by the intensity of the material heterogeneity, in particular the stronger the heterogeneity the lower is the attenuation of the high frequency components.
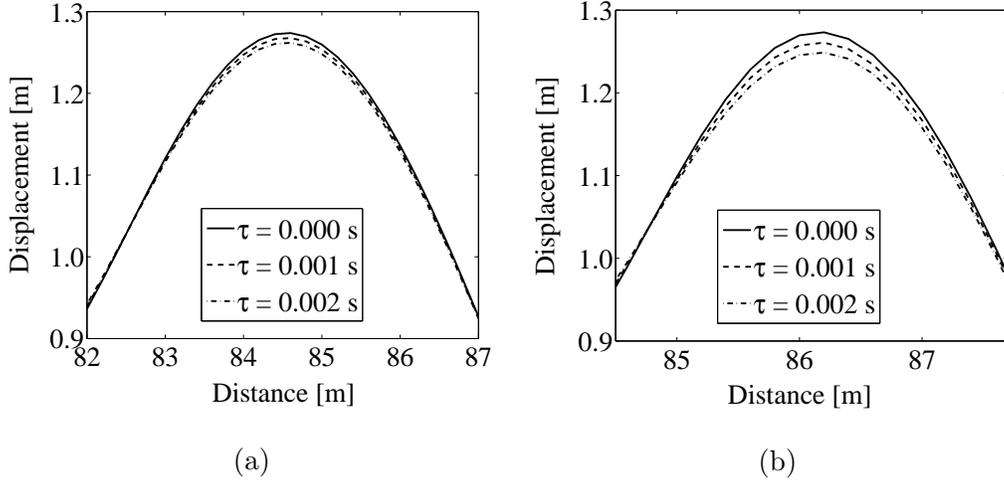
Figure 7. Effect of viscosity on the dynamic response of the bar: particular of the first peak of the wave front profile for Case a (a) and Case b (b).

Hence, as summarised in Table 1, the introduction of a gradient enrichment has a strong effect on the speed propagation of the wave front, allowing a more accurate description of the dispersive behaviour of both elastic and visco-elastic heterogeneous materials, while the viscosity has a moderate damping effect on the high frequency components and no significant effects on the speed propagation of the wave front. Therefore, the benefit of the proposed theory is that it allows, without significant additional computational costs, a more accurate description of the global dynamic behaviour of a visco-elastic material, which is not possible by applying either gradient elasticity or classical visco-elasticity alone, because of the complementary nature of the effects of gradient enrichment and viscosity.

Table 1. Entity of the effects of gradient enrichment and viscosity on both speed propagation of the wave front and high frequency components.

	Gradient enrichment	Viscosity
Speed propagation of the wave front	Strong reduction	Negligible
High frequency components	Negligible	Moderate damping

7. Conclusions

An inertia-gradient viscoelastic theory has been proposed for the mono-dimensional wave propagation problems in the case of proportional damping.

This theory represents a first attempt to extend and generalise gradient theories to the class of visco-elastic problems, and provides a more accurate tool to describe the dispersive behaviour of periodic visco-elastic composites.

The performed dispersion analysis has shown that the introduction of a micro-inertia gradient enrichment, in the governing equations, helps capturing with higher accuracy the dispersive behaviour of the discrete model; furthermore from the mentioned analysis it has been also found that by changing the value of the (stiffness-)proportional damping coefficient τ it is possible to introduce super-critical damping and, in this case, control which wave numbers are super-critically damped.

Interaction between viscosity and inertia-gradient has been also investigated as well as their effects on wave front propagation/dispersion.

The ability of the proposed theory to adequately describe dispersive wave propagation phenomena has been shown and it has been observed that vis-

23

cosity and gradient enrichment have two complementary effects, which makes essential the use of a gradient visco-elastic theory, for an accurate description of the overall dynamic behaviour of a visco-elastic material: while viscosity attenuates the high frequency components, gradient enrichment reduces the speed propagation of the wave front. Furthermore, the presented theory shows a very good agreement, in terms of displacements, with the correspondent heterogeneous model, where the microstructural heterogeneity of the material is explicitly modelled.

Since the proposed theory represents the first attempt to introduce viscosity in a gradient elasticity theory, at this stage our main goal is to explore and understand the interaction between viscosity and inertia-gradient, as well as their effects on wave dispersion rather than propose a complete gradient viscoelasticity theory; for this reason we have focused our efforts in studying a very specific problem.

Some issues remain open for future studies, in particular:

- extension of the proposed theory to periodic composites, whose constitutive materials are characterised by either proportional damping with different factor of proportionality or non proportional damping;

- extension of the one-dimensional theory to the multi-dimensional case.

AppendixA. Stability

When the argument of the square root in Eq. (22) is negative, ω_h takes the following form

$$\omega_h = \pm \mathrm{i} \frac{c_e k}{\sqrt{1 + \frac{1}{12} d^2 k^2}} \sqrt{\frac{c_e^2 k^2 \tau^2}{4 \left(1 + \frac{1}{12} d^2 k^2\right)} - 1} \qquad (A.1)$$

Considering Eq. (13), Eq. (19) can then be rewritten as

$$u(x,t) = U \exp((\mathrm{i}\omega_h - \omega_d)\, t) \exp(-\mathrm{i}kx) \tag{A.2}$$

and substituting Eqs. (21) and (A.1) into Eq. (A.2), the following expression is obtained

$$u(x,t) = U \exp\left(\left(\pm\frac{c_e k}{\sqrt{1 + \frac{1}{12}d^2 k^2}}\sqrt{\frac{c_e^2 k^2 \tau^2}{4\left(1 + \frac{1}{12}d^2 k^2\right)} - 1} - \frac{c_e^2 k^2 \tau}{2\left(1 + \frac{1}{12}d^2 k^2\right)}\right) t\right) \exp(-\mathrm{i}kx) \tag{A.3}$$

Focusing the attention on the argument of the first exponential term, it can be observed that negative values produce stable results and represent the condition of super-critical damping, while positive values would lead to unstable results (amplification of the response). However, it can easily be shown that the considered argument is always negative; hence there are no risks to incur in instabilities of the solution.

Acknowledgements

References

[1] E. C. Aifantis, On the role of gradients in the localization of deformation and fracture, International Journal of Engineering Science 30 (10) (1992) 1279–1299. doi:10.1016/0020-7225(92)90141-3.

[2] S. Altan, E. C. Aifantis, On the structure of the mode III crack-tip in gradient elasticity, Scripta Metallurgica et Materialia 26 (1992) 319–324.

[3] C. Q. Ru, E. C. Aifantis, A simple approach to solve boundary-value problems in gradient elasticity, Acta Mechanica 101 (1993) 59–68. doi:10.1007/BF01175597.

[4] E. C. Aifantis, On the microstructural origin of certain inelastic models, ASME Journal of Engineering Materials and Technology 106 (4) (1984) 326–330.

[5] E. C. Aifantis, The physics of plastic deformation, International Journal of Plasticity 3 (3) (1987) 211–247.

[6] H. Mühlhaus, E. C. Aifantis, A variational principle for gradient plasticity, International Journal of Solids and Structures 28 (7) (1991) 845–857.

[7] R. de Borst, H. Mühlhaus, Gradient-dependent plasticity: formulation and algorithmic aspects, International Journal for Numerical Methods in Engineering 35 (3) (1992) 521–539. doi:10.1002/nme.1620350307.

[8] E. C. Aifantis, Gradient effects at macro, micro, and nano scales, Journal of the Mechanical Behavior of Materials 5 (1994) 355–375.

[9] E. C. Aifantis, Gradient deformation models at nano, micro, and macro scales, ASME Journal of Engineering Materials and Technology 121 (1999) 189–202.

[10] M. Y. Gutkin, E. C. Aifantis, Dislocations and disclinations in gradient elasticity, Physica Status Solidi (b) 214 (1999) 245–284.

[11] M. Y. Gutkin, E. C. Aifantis, Dislocations in the theory of gradient elasticity, Scripta Materialia 40 (1999) 559–566.

[12] M. Y. Gutkin, Nanoscopics of dislocations and disclinations in gradient elasticity, Reviews on Advanced Materials Science 1 (2000) 27–60.

[13] M. Rubin, P. Rosenau, O. Gottlieb, Continuum model of dispersion caused by an inherent material characteristic length, Journal of Applied Physics 77 (1995) 4054–4063.

[14] W. Chen, J. Fish, A Dispersive Model for Wave Propagation in Periodic Heterogeneous Media Based on Homogenization With Multiple Spatial and Temporal Scales, Journal of Applied Mechanics 68 (2) (2001) 153–161. doi:10.1115/1.1357165.

[15] A. Metrikine, H. Askes, One-dimensional dynamically consistent gradient elasticity models derived from a discrete microstructure. Part 1: generic formulation, European Journal of Mechanics - A/Solids 21 (2002) 555–572.

[16] H. Askes, A. Metrikine, One-dimensional dynamically consistent gradient elasticity models derived from a discrete microstructure. Part 2: static and dynamic response, European Journal of Mechanics - A/Solids 21 (2002) 573–588.

[17] P. Gudmundson, Modelling of length scale effects in viscoelastic materials, European Journal of Mechanics - A/Solids 25 (2006) 379–388.

[18] H. Askes, E. C. Aifantis, Gradient elasticity in statics and dynamics: An overview of formulations, length scale identification pro-

cedures, finite element implementations and new results, International Journal of Solids and Structures 48 (13) (2011) 1962–1990. doi:10.1016/j.ijsolstr.2011.03.006.

[19] H. Askes, A. Suiker, L. Sluys, A classification of higher-order strain-gradient modelslinear analysis, Archive of Applied Mechanics 72 (2-3) (2002) 171–188. doi:10.1007/s00419-002-0202-4.

[20] I. M. Gitman, H. Askes, E. Kuhl, E. C. Aifantis, Stress concentrations in fractured compact bone simulated with a special class of anisotropic gradient elasticity, International Journal of Solids and Structures 47 (2010) 1099–1107.

[21] J. Crank, P. Nicolson, A practical method for numerical evaluation of solutions of partial differential equations of the heat conduction type, Proceedings of the Cambridge Philosophical Society 43 (1) (1947) 50–67.

[22] N. M. Newmark, A method of computation for structural dynamics, Journal of the Engineering Mechanics Division ASCE 85 (1959) 67–94.

[23] G. L. Goudreau, R. L. Taylor, Evaluation of numerical integration methods in elastodynamics, Computer Methods in Applied Mechanics and Engineering 2 (1972) 69–97.

[24] T. Bennett, I. M. Gitman, H. Askes, Elasticity Theories with Higher-order Gradients of Inertia and Stiffness for the Modelling of Wave Dispersion in Laminates, International Journal of Fracture 148 (2) (2007) 185–193. doi:10.1007/s10704-008-9192-8.